JOURNAL OF MATERIALS SCIENCE 27 (1992) 3856–3868

Mechanical response and structural development during the hot extrusion of a rapidly solidified Al–20Si–7.5Ni–3Cu–1Mg alloy powder

J. ZHOU, J. DUSZCZYK, B. M. KOREVAAR
Laboratory for Materials Science, Delft University of Technology, Rotterdamseweg 137, 2628 AL Delft, The Netherlands

The consolidation of an air-atomized Al–20Si–7.5Ni–3Cu–1Mg alloy powder was performed utilizing hot extrusion, to determine its extrudability and understand its structural development in relation to process parameters. One of the main features exhibited by the material in this process was a high degree of softening over a peak extrusion pressure, which has been explained by the simultaneous onset of dynamic recovery and recrystallization during deformation. The peak extrusion pressure was shown to be strongly dependent upon the temperature applied, and this dependence has been described with temperature compensated strain rate. It was also observed that the process parameters had a fairly narrow range applicable to the extrusion of the powdered alloy and a significant influence on the deformation behaviour of the powder particles. The combination of heating and deformation, primarily used to convert the loose powder particles into an engineering material, resulted in the decomposition of the meta-stable aluminium matrix and transformations of constituent phases, initially formed in the rapidly solidified powder. Additionally, it was found that the extrusion temperature had an effect on the lattice size and perfection of the as-extruded matrix in the material. Three intermetallic dispersoids containing nickel were detected in the consolidated material, independent of extrusion temperature, and their formation was promoted by hot deformation. The silicon crystal phase in the extruded material was reshaped, and its size was insensitive to the extrusion temperature, which is thought to be caused by a high volume fraction of the co-existent dispersoids. The dispersions of the silicon crystals and intermetallic compounds with various sizes in the matrix substantially modified the deformation mode of the alloy. Evidence of dynamic recrystallization was found, which co-operated with dynamic recovery during deformation, giving rise to a duplex microstructure in the extruded material.

1. Introduction

Modern, light-weight components in automotive engines and compressors require an aluminium alloy with high dimensional stability, good wear resistance, and adequate room and elevated temperature strengths. The simultaneous requirements of the physical and mechanical properties inevitably lead to the involvement of a number of additives in the alloy, all of which play their own parts in establishing the desired properties. The complicated composition of a newly designed Al–20Si–7.5Ni–3Cu–1Mg alloy clearly embodies the desire of the alloy developers to satisfy all these requirements [1]. The very heavy alloying, however, makes the conventional ingot casting technique unsuitable to produce the alloy with the necessary, fine dispersions of closely spaced silicon crystals and dispersoid phases. In this case, producers have to resort to the technique of powder metallurgy [2], which is known for overcoming a number of shortcomings associated with the ingot metallurgy. With this technique, the material is first atomized into a powder form. Thanks to the involvement of rapid solidification in atomization, the powdered alloy usually has a fine microstructure and a homogeneous composition distribution. It is obvious that, however advantageous the initial microstructure produced by atomization is, the achievement of the desired properties can only be realized when the atomized powder is appropriately consolidated into an engineering material. Understanding and controlling the hot extrusion of the powder, as an efficient means of consolidation, are therefore of great importance for alloy development, process technology, as well as material applications. However, no work has so far been reported on the consolidation of this quinary alloy.

The present investigation is a part of a systematic study on the Al–20Si–7.5Ni–3Cu–1Mg alloy. A preceding investigation on the atomized powder [3] has

0022–2461

shown that structural inhomogeneities, though on a micro scale, appear within and between the powder particles due to the operation of differing solidification mechanisms during powder production. Diminishing the inhomogeneities by exerting appropriate deformation to the powder is an important factor in ensuring satisfactory properties of the material. It has also been shown that the aluminium matrix and other constituent phases in the powdered alloy are in meta-stable states. In such a case, structural changes can be expected to occur during pre-heating and during extrusion, and in turn to affect the deformation behaviour of the material. Obviously, obtaining a basic understanding of the structural evolutions in relation to the process parameters of extrusion is of use for improved control of the process and the resultant properties of the material.

Based on the previous observations, the objectives of the present work on the consolidation of the powder were: (i) to characterize the pressure variation during extrusion and describe the relationship between pressure requirement and process parameters; (ii) to assess the extrudability of the powdered alloy; (iii) to understand the structural evolutions of the aluminium matrix and constituent phases, and (iv) to determine the deformation mode and account for the mechanical response of the alloy during extrusion.

2. Experimental procedure

The raw material in the form of an air-atomized powder was supplied by the Showa Denko K. K., Japan. An analysis showed the composition of the powder to be 19.30 wt %Si, 7.57 wt %Ni, 3.24 wt %Cu, 1.18 wt %Mg and the balance aluminium. For the other basic data of the powder including oxygen content, surface oxide layer thickness, specific surface area, size and size distribution, and morphology, the reader is referred to preceding publications [3, 4]. In the present work, the powder was hot consolidated using a 2 MN horizontal extrusion press, which has been described in detail elsewhere [5]. Extrusion temperatures applied ranged from 325–475 °C, and reduction ratios from 5:1–60:1. Ram speed was kept at 5 mm s^{-1}. Flat dies producing the required reduction ratios were used and their temperature was preset at 50 °C below the pre-heating temperature of the press liner. Before extrusion, the powdered billets were heated in the liner for 20 min. During extrusion, the variation of pressure as a function of ram displacement was recorded. In the mean time, the frictions at the die and liner inner surfaces were measured. They consistently showed very low values in comparison with the extrusion force, partly owing to the application of a lubricant. Their influence on the total extrusion pressure was thus slight, so that the extrusion pressure could be regarded as a measure of the internal resistance of the material to deformation. After extrusion, the consolidated material was cut off the discards and quenched in water. Some extrusion operations were stopped to examine the behaviour of the original powder particles in the course of the deformation with optical microscopy. The material extruded at different temperatures was analyzed by means of X-ray diffractometry to obtain information on the aluminium matrix lattice and to identify phases formed in the material. A Siemens type F-ω powder diffractometer was used with copper radiation at 45 kV and 30 mA. The analysis was done at 24 °C. Both transverse and longitudinal sections of the extrudates were examined using scanning and transmission electron microscopy (SEM and TEM). SEM specimens were heavily etched and covered with a gold layer. Observation was made in a Jeol JXA 50 A scanning electron microscope with the attachment of an X-ray energy dispersive system (EDS). TEM disc specimens were thinned with an ion mill operating at a beam current of 0.5 mA and a gun inclination angle of 20°. A Philips EM 400 transmission electron microscope working at 120 kV was employed for observation.

3. Results and discussion

3.1. Extrusion characteristics

Fig. 1 shows the representative variations of the extrusion pressure with ram displacement, exhibited by the initially powdered material at the reduction ratio of 20:1 and different extrusion temperatures. Apart from a number of typical features of powder extrusion, which have been described at length elsewhere [5], it was observed that the drop of pressure from a peak value to a steady state was extraordinarily great, the steady-state pressure being only about 40% of the peak pressure. This is a clear mechanical response arising from a very high degree of softening as soon as the resistance of the material to deformation attained its maximum. Such a large pressure reduction is in agreement with the observation of a duplex microstructure consisting of dynamically recovered and recrystallized grains in the extruded material, which will be shown later. Hence, the operation of dynamic restoration is considered to be a major cause for this softening. Another factor that may also be related to the softening is the dynamic precipitation from the meta-stable aluminium matrix. This may be particularly true at low extrusion temperatures where precipitation during pre-heating does not take place to the full, the evidence of which will be given later.

A comparison with the extrusion behaviour of the base alloy without the nickel addition (Al–20Si–3Cu–1Mg) [5] showed an increased pressure requirement for extruding the present alloy, indicating an increased resistance to deformation resulting from the inclusion of additional nickel-containing phases in the material. The comparison also showed that the present nickel-containing alloy exhibited higher rates of work hardening and softening. It appears that the silicon crystals and nickel-bearing intermetallic compounds, having formed in the material being extruded, acted as effective obstacles to dislocation motion at the early stage of deformation, which resulted in a quick increase of external pressure to carry on the continuing deformation. Once the pinning by the obstacles was overcome, the material was greatly softened by a dynamic recovery mechanism. Moreover, as will be shown later, the difficulties with dislocation

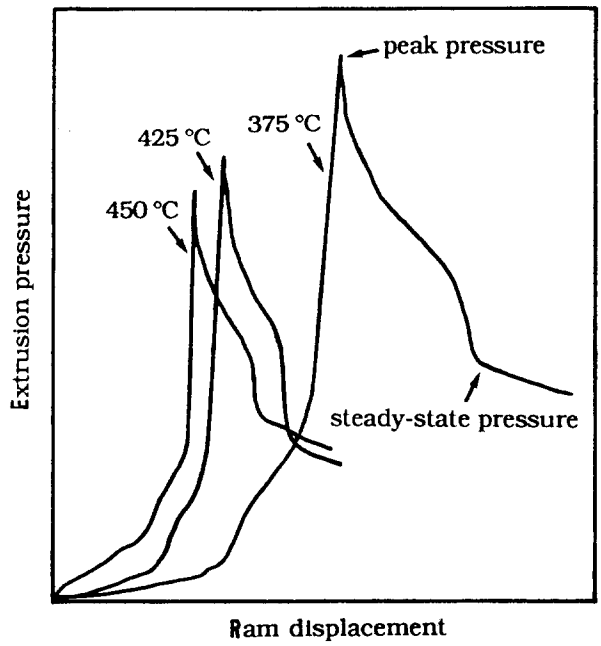

Figure 1 Extrusion pressure/ram displacement diagrams exhibited by the material at different temperatures; reduction ratio 20:1, ram speed 5 mm s^{-1}.

motion imposed by the internal obstacles promoted local recrystallization to occur, which further accelerated the softening of the material.

Additionally, a comparison between the part of the pressure/ram displacement curves before the attainment of the peak values (Fig. 1) showed a slight increase in slope with rising temperature, which means that the material extruded at a higher temperature was more quickly work hardened. Such an observation is not consistent with the usual understanding that at a higher temperature a material has a lower work hardening rate. One of the major factors, which may account for the unusual variation observed, is the retention of the alloying elements in the aluminium matrix. At the low extrusion temperature of 375 °C, the precipitation of silicon and magnesium from the initial supersaturated matrix was completed during the heating before extrusion, but the precipitation of nickel and copper (which tied one another) was not, as indicated by a thermal analysis of the powder using differential scanning calorimetry (DSC) [3]. Because a part of nickel and copper remained dissolved in the aluminium matrix, the number and interspacing of dispersoids as internal obstacles to metal flow would not be sufficient to result in a very high work hardening rate. At the higher temperatures, though increased amounts of equilibrium solutes, magnesium and silicon, were allowed to be retained in the solid solution and dynamic restoration was more easily activated, the full precipitation of copper and nickel, however, occurred during the heating prior to deformation, thereby placing more closely spaced obstacles to metal flow in the material. This would enhance the work hardening rate of the material at the higher temperatures.

The other characteristics exhibited by the present alloy during extrusion were a strong dependence of the peak pressure on temperature and a narrow usable temperature range. In the experiments, the extrusion at 325 °C failed in execution, because at this temperature the peak extrusion pressure went beyond the permissible power capacity of the press. This high pressure requirement is clearly caused by strong work hardening before the onset of dynamic restoration. Another cause, which may be of minor importance, is strain precipitation. According to the behaviour of the powdered alloy in a heating process [3], the structural evolutions of the meta-stable matrix and dispersoid phases are incomplete during heating up to 325 °C and should therefore continue during subsequent deformation. To assist the structural evolutions, an additional strain energy and thus a raised external pressure will be required [6]. The operation reached an upper limit at 475 °C where an extrusion defect, hot shortness, started to appear. As the alloy begins melting at 520 °C, the appearance of the hot shortness indicates that the temperature rise, resulting from deformation and friction, exceeded the temperature margin available. Obviously, the exhibited lower and upper limits substantially narrow the temperature range usable for the extrusion of the alloy, and the results reported below are restricted to the extrusion over the temperature range of 375–450 °C.

As shown earlier, the work hardening degree of the material is sensitive to the temperature applied. Correlating the peak extrusion pressure with process parameters is, therefore, of practical importance, because this pressure is a breakthrough value determining whether the execution of an extrusion is possible. It was found that, over the temperature range of 375–450 °C, the peak extrusion pressure decreased steadily with rising temperature without showing a sudden change, which suggests that the work hardening and softening mechanisms operating in the material during extrusion did not differ very much. Fig. 2 shows a plot of the peak extrusion pressure against the reciprocal absolute temperature. It has been established [5] that, when reduction ratio and ram speed are constants, the peak extrusion pressure, p, can be

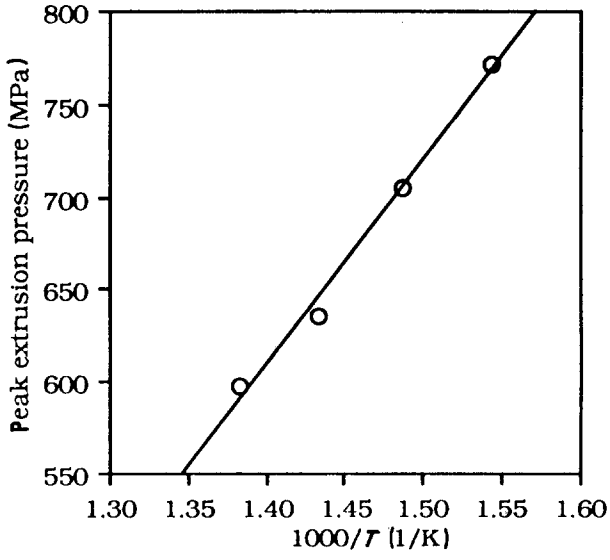

Figure 2 Plot of the peak extrusion pressure against the reciprocal absolute temperature.

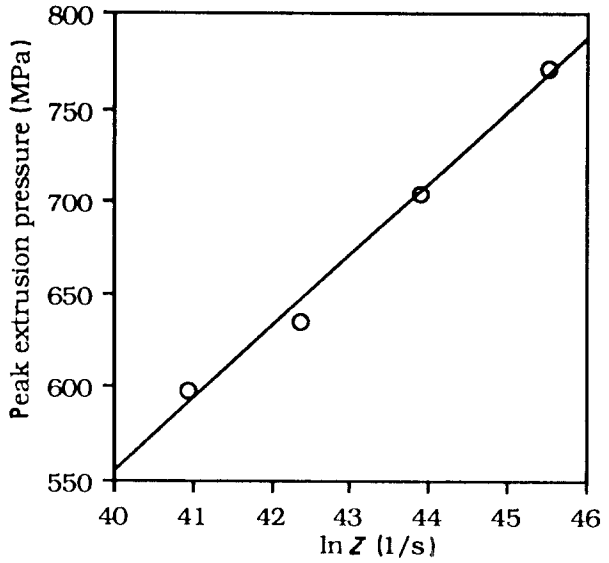

Figure 3 The peak extrusion pressure as a function of the logarithm of the temperature-compensated strain rate.

described by

$$p = a + b\ln Z \quad (1)$$

where a and b are constants, and Z is temperature-compensated strain rate defined as

$$Z = \dot{\varepsilon}\exp(\Delta H/RT) = A[\sinh(\alpha\sigma)]^{n'} \quad (2)$$

where $\dot{\varepsilon}$ is the mean strain rate, ΔH the activation energy for deformation, R the universal gas constant, T the absolute temperature, A, α and n' are material constants, and σ is effective flow stress. For a given reduction ratio and ram speed, the mean strain rate $\dot{\varepsilon}$ is also an invariable. We can then combine Equations 1 and 2, arriving at

$$p = c + b\Delta H/RT \quad (3)$$

where c is a new constant. Equation 3 shows a linear relationship between p and $1/T$, which is in good agreement with the plot given in Fig. 2. This demonstrates the validity of the empirical Equation 1 for the extrusion of the present alloy. The activation energy for deformation ΔH in Equation 2 was determined by torsion tests on the material at different temperatures and strain rates. A value of 233 kJ mol^{-1} was obtained. With this value, we calculated the temperature-compensated strain rates and related them to the variation of the peak extrusion pressure, as shown in Fig. 3. It is clear that the peak extrusion pressure increases linearly with the rising logarithmic temperature-compensated strain rate.

3.2. Deformation of powder particles

It has been reported that, in rapidly solidified Al–Fe alloy powders, an inhomogeneous microstructure responds non-uniformly to applied stresses. Some very fine powder particles are strong enough to resist deformation during extrusion in certain conditions [7]. This is consistent with the measured differences in the microhardness of the inhomogeneous microstructure (which can be larger than a factor of 2 [8, 9]). In the present Al–Si–Ni–Cu–Mg alloy powder, a broad range of microstructures, varying within and between the powder particles, has been observed [3]. It is hence of interest to examine the behaviour of the powder particles during extrusion under varying conditions. Obviously, a proper set of extrusion parameters should produce applied stresses far in excess of the yield stress of each powder particle so that all of the powder particles can be distorted. In this case, the internal structure of each powder particle will be affected and the initial inhomogeneities can be lessened. Fig. 4 illustrates the deformation behaviour of the powder particles, which is very sensitive to the process parameters. Fig. 4a shows a structure extracted from the rear part of a billet partially extruded at a temperature of 375 °C and reduction ratio of 20:1, as indicated in Fig. 4e. It can be seen that intimate contacts between the powder particles have been attained, probably by mutual sliding and tilting, but their initial shapes remain practically unaffected. Note that, under this extrusion condition, the pressure exerted on the back of the billet was about three times as high as the peak flow stress of the consolidated material calculated from Equation 2, in which the material constants, A, α and n', were determined by using hot torsion as simulative deformation. This indicates that the compression pressure, though very high, could not bring about large deformation. Fig. 4b shows a structure of the material which was worked under the same condition and extracted from the extruded part. It can be observed that the powder particles have been extensively elongated, independent of their initial shapes or sizes, indicating that the resultant shear stresses, closely related to the applied temperature and reduction ratio, were sufficiently high to destroy the original powder particle characteristic. When a high temperature (450 °C) and a low reduction ratio (5:1) were used, which corresponded to a low value of temperature-compensated strain rate, Z, however, a few very fine, hard powder particles remained undeformed, as shown in Fig. 4c. Also, when a high Z value (such as a reduction ratio of 60:1 and a temperature of 375 °C) was applied, another problem arose. Some coarse primary silicon crystals cracked and their compatibility with the aluminium matrix became imperfect, which is clearly illustrated in Fig. 4d. This is probably because the temperature and thus the metal flow of the matrix were not high enough to close the voids between the cracked silicon crystals. These unclosed voids are potentially detrimental to the mechanical properties of the material. It is, therefore, of great importance to optimize the processing conditions by adjusting the process parameters, mainly temperature and reduction ratio. As shown above, their combined effect can be reflected by the temperature-compensated strain rate, Z, and hence an appropriate process condition can be set by adjusting this parameter.

3.3. Precipitation and transformation

The results previously obtained from thermal and X-ray diffraction analyses have shown that the atomized powder before consolidation contains the

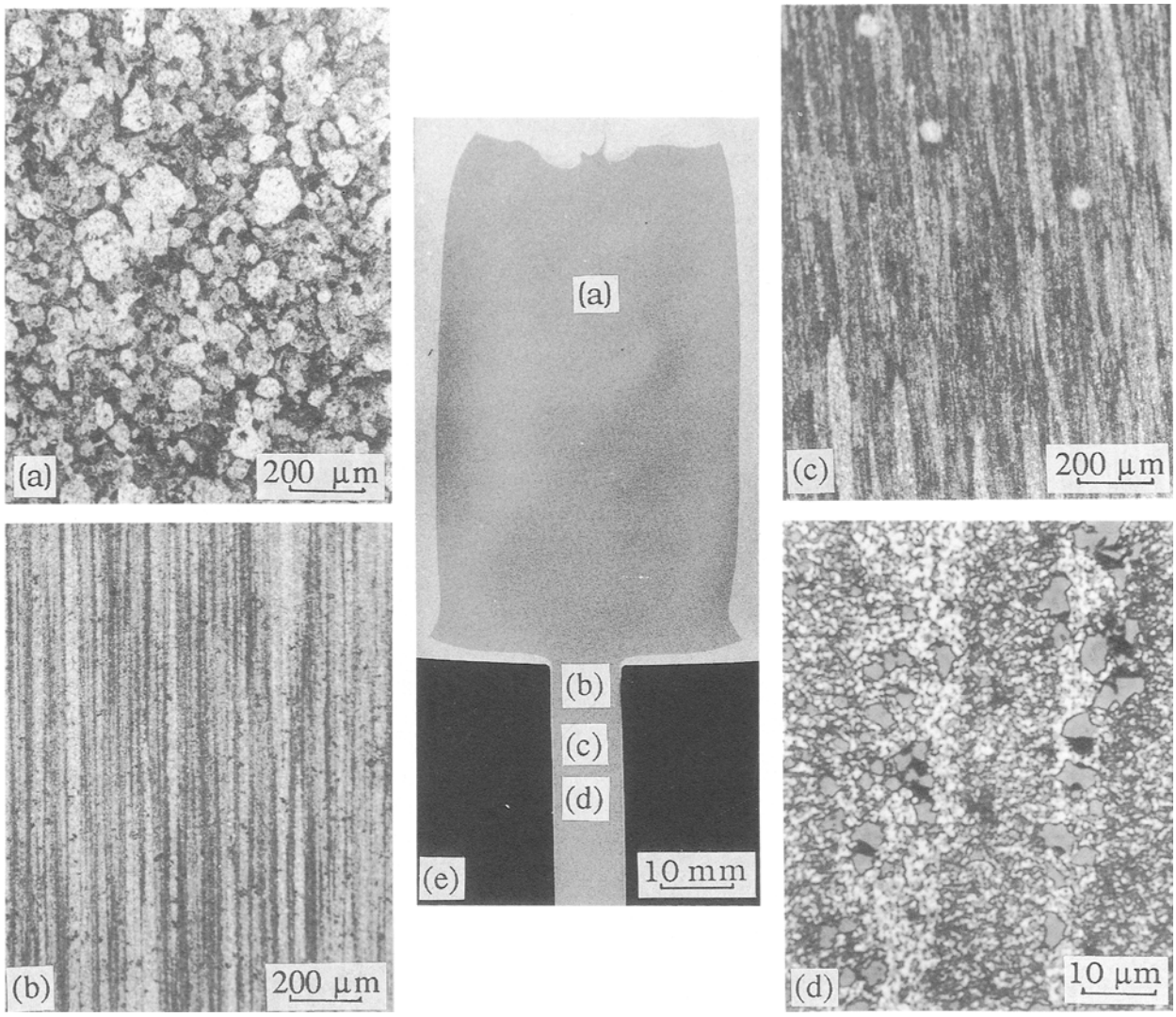

Figure 4 Deformation of the powder particles under different extrusion conditions: (a) a retained powder structure in the rear part of a partially extruded billet (375 °C/20:1); (b) a heavily distorted powder structure after deformation (375 °C/20:1); (c) an extruded structure containing undeformed powder particles; (d) cracked silicon crystals in an extruded microstructure (375 °C/60:1), and (e) a partially extruded billet showing the locations of the micrographs taken.

meta-stable aluminium matrix, silicon crystals and intermetallic phases [3]. Apparently, during pre-heating and during subsequent deformation, the meta-stable material has a strong propensity to attain its equilibrium state by precipitating solutes from the supersaturated matrix and transforming non-equilibrium compounds into equilibrium ones. To limit the number of process variables, the work reported below on the structural evolutions during extrusion takes the extrusion temperature as a prime process parameter, which varies between 375 and 450 °C, while the reduction ratio is fixed at 20:1.

Fig. 5 presents comparisons of the diffraction lines from the reflection plane {4 2 2} of the matrices of the material extruded at different temperatures and of the powder. It was noted that the asymmetry of the diffraction line as exhibited by the matrix of the powder, which has been explained to be caused by the non-uniform supersaturation of the solute atoms in the matrix [3], was greatly lessened. After extrusion, the peaks tended to be resolved into doublets of K_{α_1} and K_{α_2}. Also, the breadths of the diffraction lines at their half maxima were substantially reduced, largely due to the precipitation of the solute atoms during pre-heating and probably also during deformation. But the diffraction lines from the extruded matrices were still broadened when compared with the line from the pure aluminium, indicating that a part of the lattice distortions was still retained in the as-extruded matrices. Additionally, the breadths exhibited by the as-extruded matrices decreased progressively with rising extrusion temperature. There are a number of possible factors responsible for the observed broadening and broadening variation. As most of the supersaturated solutes were already precipitated out after the extrusion over the temperature range (which has been confirmed by a thermal analysis of the extruded material), the effect of the retained solutes on the lattice distortions of the matrices would not be significant. The difference in thermal shrinkage between the aluminium matrix and the silicon crystals should then be principally responsible for the observed broadening of the diffraction lines from the as-extruded matrices [10]. This factor, however, does not fully account for the decrease of the breadth with rising extrusion temperature. The retained internal

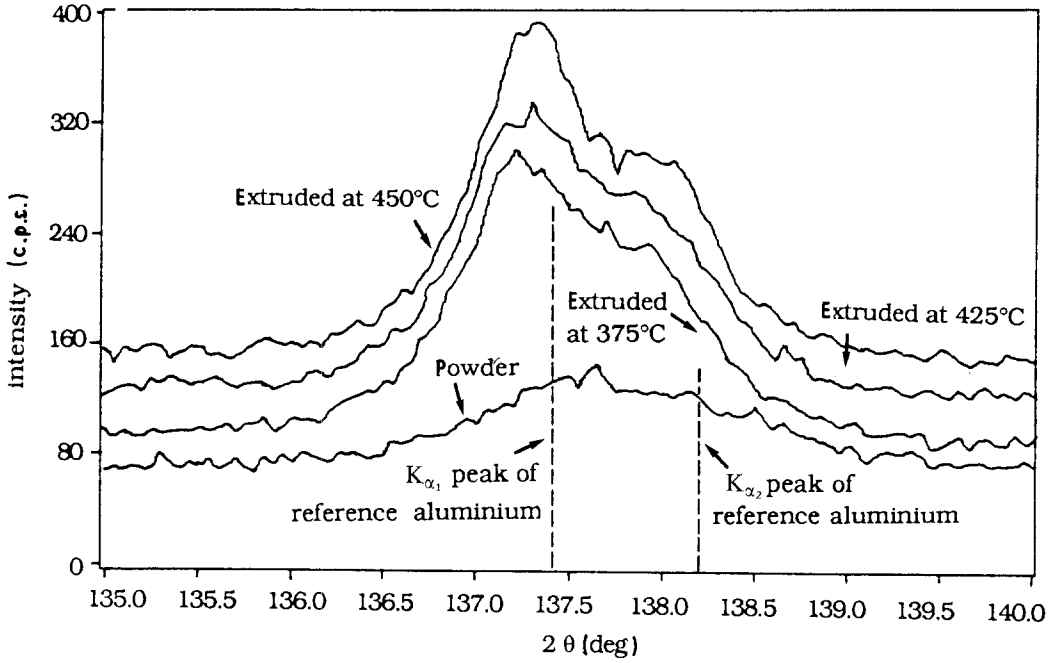

Figure 5 X-ray diffraction lines from the matrices in the material extruded at different temperatures in comparison with the line from the matrix in the powder using CuK_α radiation and a reflection plane of {4 2 2}.

stresses and strains resulting from heavy deformation are considered to be associated with the variation of the breadth. This is understandable because the lattice defects such as dislocations, if not fully eliminated by complete restoration, will lead to the imperfection of the matrix lattice and thus the broadening of diffraction lines. In the present alloy, very high volume fractions of silicon crystals, dispersoids and precipitates are present in the aluminium matrix being deformed, and they undoubtedly resist restoration during and after deformation. At a higher extrusion temperature, more dislocations can be thermally activated to annihilate or move to the sinks like grain and subgrain boundaries. Or more recrystallized grains with reduced dislocation densities will be created. As a result, the retained dislocation density in the grains of the aluminium matrix extruded at a higher temperature is lower, which leads to a less broadened peak of the diffraction line. It is, therefore, concluded that the observed broadening of the diffraction lines is mainly due to these two factors: the difference in thermal expansion coefficient between the aluminium matrix and silicon crystals, and the lattice defects retained after extrusion.

Average lattice parameters of the as-extruded matrices were calculated from the K_{α_1} reflection after separation from the K_{α_2} component. They showed increased values as compared with the lattice size of the matrix in the powder. The increase is apparently ascribable to the precipitation of the supersaturated solutes: nickel, copper, and silicon, which tend to decrease the lattice size of aluminium and are capable of overcoming the reverse effect given by magnesium. The calculation also showed that the average lattice parameter of the aluminium matrix in the material decreased from 0.40525 to 0.40519 nm over the extrusion temperature range from 375 to 450 °C. If the influence of the X-ray diffractometer (which was set in identical conditions) on the accuracy of the measurements is left out of consideration, the variation can be ascribed to the resolution of the alloying elements in the aluminium matrix. Nickel has a very limited equilibrium solid solubility in aluminium (being 0.01 at % at 500 °C in the Al–Ni binary system [11]) and its variation over the extrusion temperature range is minute, so that the effect of nickel can be neglected. Among the solvable elements: silicon, copper and magnesium, only magnesium tends to increase the lattice size of aluminium. It is known that, when both silicon and magnesium are in the solution, the over-all effect is to decrease the lattice size of aluminium [12]. Even if the effect of copper is not taken into account, which is in fact strongly tied with nickel [3, 12], the combined effect of silicon and magnesium can explain the observed variation of the aluminium matrix lattice size with extrusion temperature. During the heating up to the extrusion temperatures, the solutes are first precipitated out, driven by supersaturation. As the equilibrium solid solubilities of silicon and magnesium increase with rising temperature, increased amounts of the solutes can be retained in the solution (the equilibrium solubilities of silicon and magnesium are almost doubled over the extrusion temperature range in the Al–Si–Mg ternary system [13]). During the relatively fast cooling from the extrusion temperatures, their precipitation does not occur for kinetic reasons. As a result, the aluminium matrix of the material extruded at a higher temperature contains larger amounts of silicon and magnesium and hence shows a smaller average lattice parameter. It is, therefore, clear that, in addition to the silicon crystals [10], the retention of the solutes, depending upon extrusion temperature, also has an influence on the lattice size of the aluminium matrix.

Fig. 6 gives an X-ray diffraction chart, summarizing the changes of the reflections from different phases in

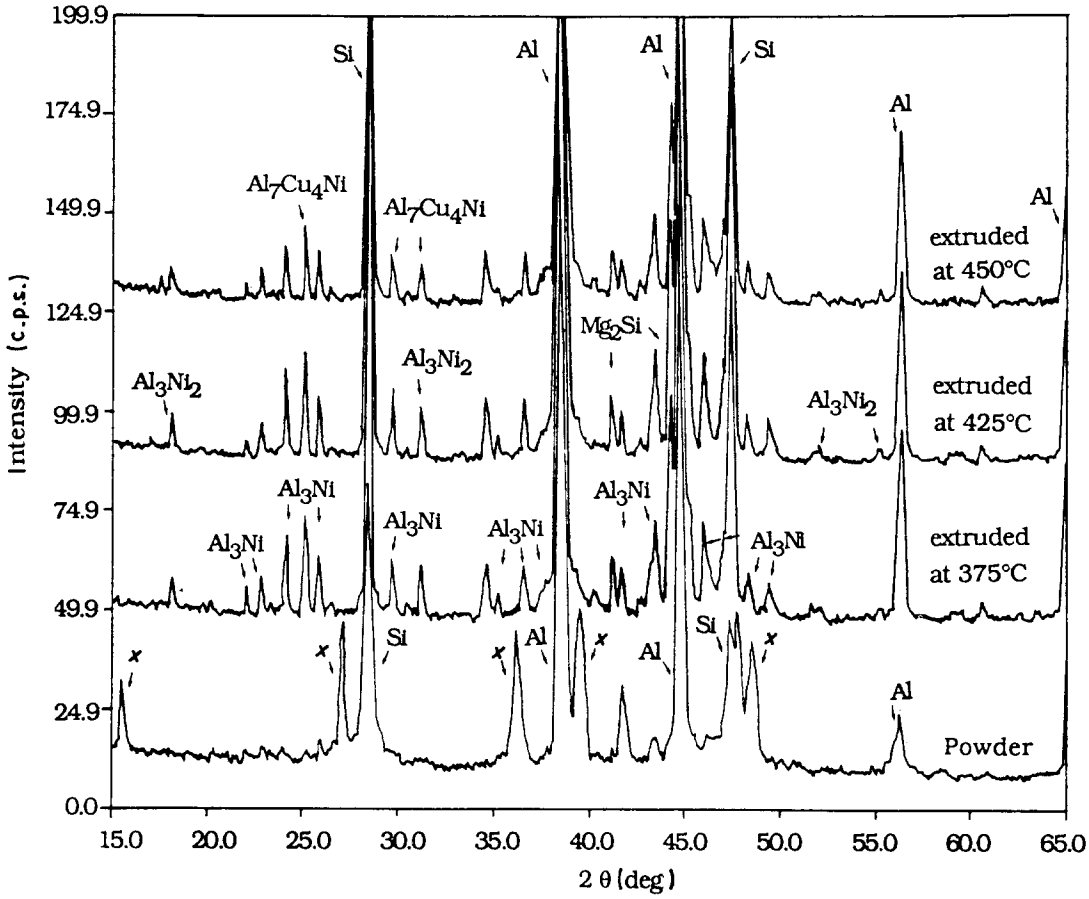

Figure 6 X-ray diffraction patterns showing the changes before and after extrusion and phase identification.

the powder and in the material extruded at three temperatures. The reflections from the meta-stable intermetallic compounds in the atomized powder (marked *x* in the chart) matched none of the established phases [3]. This means that the intermetallic phases were in meta-stable states and with non-stoichiometric compositions. After extrusion, all the reflections could be indexed and assigned to the phases indicated in the chart. It is clear from the chart that, for the material extruded at temperatures of 375–450 °C, no differences in the reflections can be recognized. This implies that the material extruded over this temperature range contained the same phases in similar amounts. It should be recalled that, in a previous investigation on the powder, the complex decomposition lasted up to above 410 °C during a DSC analysis [3]. In the present work, a DSC analysis of the material extruded at 375 °C showed no sign of the resumption of decomposition or transformation, but only of continuing resolution with rising temperature, indicating that the material extruded at 375 °C had already attained its equilibrium condition. A comparison of the behaviour of the material before and after extrusion in the thermal analysis suggests that the decomposition of the meta-stable matrix and the formation of intermetallic compounds were promoted to a certain extent by deformation, at least during the extrusion at 375 °C, and that dynamic precipitation was indeed involved in the extrusion of the alloy.

The phases present in the extruded material are equilibrium ones except Mg_2Si which has a hexagonal structure and is a meta-stable phase. Such an intermediate phase (often designated as β′ phase) normally appears at a certain stage of ageing [12, 14]. Its presence in the present extruded material is interesting. It could form by precipitation from the meta-stable matrix during the heating prior to extrusion in a static manner. Dynamic formation of this phase is, however, also possible, either by precipitation directly from the meta-stable aluminium matrix or by transformation from the equilibrium Mg_2Si phase with a face centred cubic structure. Similar dynamic precipitation has been observed in an Al–Cu alloy and other alloys and explained in terms of the assistance by point defects and dislocations of high densities created by large deformation [15, 16]. Also, dynamic transformation of the Mg_2Si phase from the face centred cubic structure to the hexagonal one has been reported [17]. Unfortunately, in a hot extrusion operation as applied to the powder, the static and dynamic processes cannot be readily separated and thus the mechanism of this phase formation cannot be ascertained in the present work.

The nickel-containing phases formed in the extruded material are well-established intermetallic compounds, but they are not very often encountered in conventional aluminium alloys. As expected, the Al_3Ni phase with an orthorhombic structure (ASTM 2–416) appeared after extrusion. Although this phase may form by precipitation directly from the meta-stable aluminium matrix, it is considered to stem mostly from a distorted parent phase with a monoclinic structure, probably Al_9Ni_2, formed through a eutectic reaction in non-equilibrium conditions [3].

This transformation has been observed in a number of investigations on rapidly solidified Al–Ni alloys [18–20] and supported by microscopy in the present work, which will be shown later. The parent Al–Ni phase is known to be thermomechanically unstable and to be transformed into the equilibrium Al_3Ni phase upon heating or even upon deformation at room temperature [19]. The appearance of the Al_3Ni phase, which should have been formed through a ternary eutectic reaction under the equilibrium conditions of solidification, indicates the completion of an equilibrium ternary phase constitution (Al–Si–Al_3Ni) in the material after hot extrusion.

As the alloy has a high silicon content (a small part of which is consumed in the Mg_2Si phase), there should be an excessive amount of silicon existing in the silicon crystal form to match the Al_3Ni phase in the ternary phase constitution. It is, therefore, considered that most of the added nickel is present in the Al_3Ni phase, as the most important dispersoid in the material. Because nickel has a very low diffusivity and solid solubility in aluminium, the Al_3Ni phase is thermally stable. Hence, this dispersoid can be expected to inhibit the motion of dislocations effectively, thereby substantially contributing to the high temperature strength of the alloy [21]. It has been reported that the Al_3Ni compound starts softening at about 300 °C [22]. This, at first sight, seems to be inconsistent with its desired contribution to the hot strength of the material. As a matter of fact, the Al_3Ni dispersoid in an aluminium alloy is incoherent with the aluminium matrix, and its strengthening is accomplished by the Orowan mechanism, which is more dependent on its size and interspacing than on its intrinsic strength [23].

Another nickel-containing compound detected is the Al_3Ni_2 phase with a trigonal structure (ASTM 14–648). Its appearance seems to be inconceivable in consideration of the equilibrium Al–Ni–Si ternary system, because this phase does not exist in the aluminium-rich corner. In the Al–Ni binary system, it emerges at a composition of 42 wt %Ni [24], which is certainly not the case for the present alloy. It is very likely that the detected Al_3Ni_2 phase is associated with the Al–Ni–Cu ternary system, in which copper is incorporated in the Al_3Ni_2 phase to form the $Al_3(NiCu)_2$ phase [12]. The third nickel-containing compound detected is the Al_7Cu_4Ni phase with a rhombohedral structure (ASTM 28–16). These two nickel- and copper-containing compounds are assumed to be largely formed by the precipitation of the supersaturated solutes, which occurred at around 410 °C during a static process [3]. Their appearance in the material extruded at 375 °C may again suggest the assistance of large deformation to their formation. The possible influence of the nickel- and copper-containing dispersoid formation on the ageing response of the alloy has been under discussion [3]. The present investigation on the extruded material supports a previous prediction that the desired precipitation on ageing may be substantially diminished. Neither Al_2Cu nor $Cu_2Mg_8Si_6Al_5$ precipitate which was initially expected, could be found in the X-ray diffraction chart obtained from the material extruded under the given conditions. This indicates that no detectable amounts of these precipitates were formed during pre-heating, or during extrusion by a strain ageing mechanism, or during cooling after deformation. Subsequently heating the extruded material in a thermal analysis did not reveal any appreciable precipitation. All the evidence suggests that a strong ageing strengthening effect, as initially desired, may be absent in the present alloy with the nickel addition.

3.4. As-extruded microstructure

Fig. 7 shows a typical optical microstructure of the material extruded at a temperature of 375 °C and reduction ratio of 20:1. As desired for the achievement of the physical and mechanical properties of the alloy, a very high volume fraction of silicon crystal phase was observed after extrusion, which was homogeneously distributed and composed of faceted, block-like and fine granular crystals. The branched silicon phase, as a constituent of eutecticum formed in the medium and fine powder particles under rapid solidification conditions [3], was no longer observable. This indicates that a significant change in the morphology and thus an increase in the number of the silicon crystals occurred in the material, driven by the tendency to reduce their surface energy, when the material was exposed to the high temperature. This change might be promoted by vacancy concentrations resulting from large deformation. A direct benefit gained from this change is that the initial microstructural inhomogeneity within and between the original powder particles is diminished. It was also noted that, under this extrusion condition, extensive fragmentation of the block-like silicon crystals did not happen. Systematic alignment of the silicon crystals in the extrusion direction as stringers was not very apparent on the longitudinal sections of the extrudate. The

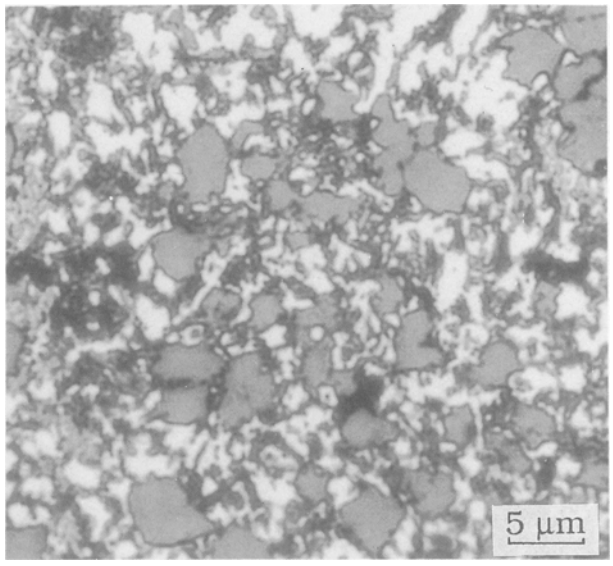

Figure 7 Optical micrograph taken from the material extruded at 375 °C/20:1.

reason for this may be that, in the material being deformed, the volume fraction of the non-deformable silicon crystals is very high which restricts the rearrangement of the silicon crystals in the softened matrix. If the applied stresses are not sufficiently high, the alignment will be limited. At a high reduction ratio, however, the alignment of the block-like silicon crystals was produced, as has been shown in Fig. 4d. In this case, the discontinuous stringers of the block-like silicon crystals will provide an easy cracking path, hence degenerating the mechanical properties of the material, especially in the transverse direction.

An EDS analysis of the phases in the extruded material showed that the matrix was almost depleted of the solutes, and that the black-coloured phase neighbouring the silicon crystal phase (Fig. 7) had a composition very close to that of the Al_3Ni phase. The location of the intermetallic phase suggests that it is very likely a product of transformation from a parent phase formed in association with silicon and aluminium-rich phases through a non-equilibrium eutectic reaction, rather than a product of decomposition from the meta-stable aluminium matrix. The products from the decomposition of the meta-stable aluminium matrix were much finer, indiscernible by optical microscopy. They preferentially formed at the interfaces between the aluminium matrix and the silicon crystals, as shown in Fig. 8 (bright particles). Because of their very fine sizes, it was difficult to analyse their compositions, avoiding contributions from the neighbouring phases. However, based on the results obtained from X-ray diffraction, as given earlier, they are very likley nickel- and copper-containing phases, $Al_3(NiCu)_2$ and Al_7Cu_4Ni.

Interestingly, the variation of the extrusion temperature over the range of 375–450 °C did not produce any recognizable difference in the sizes of the silicon crystals and Al_3Ni dispersoids. The insensitivity of the Al_3Ni dispersoid size to the extrusion temperature can easily be understood in view of its high thermal stability. For the silicon crystals, however, a definite dependence of their size on extrusion temperature has been observed in the Al–Si–Cu–Mg base alloy [25]. At extrusion temperatures above 400 °C, the coarsening of the silicon crystals is obvious, primarily because silicon has a relatively high solid solubility and diffusion coefficient in aluminium. It may be assumed that the mechanism of the coarsening of the silicon crystal phase is by atomic diffusion from dissolving crystals through the aluminium matrix to growing ones. In the base alloy, almost no thermally stable internal particles can effectively hinder the diffusion to take place at the extrusion temperatures where many of the copper- and magnesium-containing precipitates are dissolved. On the other hand, extrusion creates subgrain boundaries to provide an easier path for the diffusion to proceed. The growth of the silicon crystals in the base alloy, therefore, becomes inevitable at high temperatures. In the present alloy with the nickel addition, however, three nickel-containing dispersoids, Al_3Ni, $Al_3(NiCu)_2$ and Al_7Cu_4Ni, are virtually insolvable at the extrusion temperatures and resident at grain and subgrain boundaries and within grains to block the diffusion of silicon atoms. Moreover, many nickel-containing dispersoids are situated at the interfaces between the silicon crystals and matrix, as shown earlier. As a result, the coarsening of the silicon crystals at the extrusion temperatures is lessened. A similar beneficial effect of dispersed intermetallic phases on the silicon crystal growth has been observed in an iron-added Al–Si–Cu–Mg alloy which shows an improved thermal stability of the silicon crystal phase during extrusion and during a heat treatment subsequent to extrusion [26].

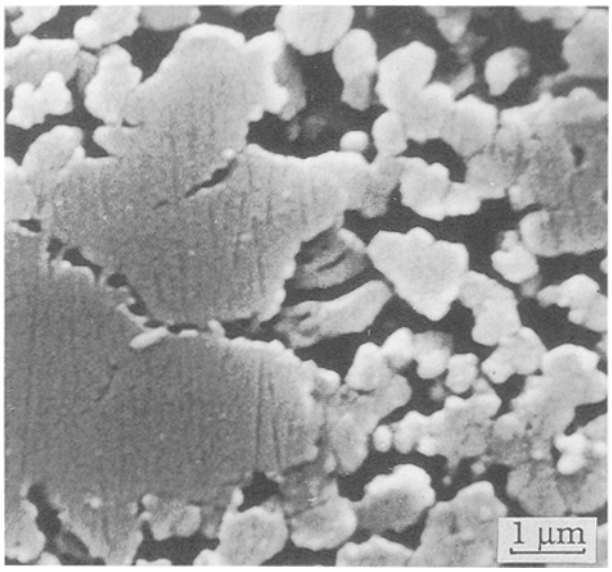

Figure 8 SEM micrograph showing the precipitates at the interface between the silicon crystals and matrix.

Fig. 9 shows electron micrographs taken from transverse sections of the material extruded at 375 °C. Fig. 9a is representative of the general microstructure composed of a mixture of subgrains and recrystallized grains. The subgrains were observed to be irregular in shape and various in size, and some contained internal dislocations and microcells. This suggests that polygonization did not go to completion during extrusion, primarily because of the difficulty of subgrain boundary migration in the alloy with high volume fractions of the silicon crystals and dispersoids. More interesting is the appearance of a number of recrystallized grains in the as-extruded microstructure, though they have a low volume fraction in comparison with the recovered grains. Fig. 9b shows a recrystallized grain with a size of about 0.8 μm, which has high misorientations with its surroundings, as indicated by high contrast. In this grain, an indistinct substructure can be seen, especially around an internal particle of about 0.05 μm. It may be argued that the substructure only appearing around the isolated internal particle does not provide hard evidence that the grain was dynamically formed during deformation. The reason is that if a potent nucleus of recrystallization was present in the material, static recrystallization and subsequent growth (termed meta-dynamic recrystallization) could occur very quickly during the time interval after deformation but before quenching. The observed substructure around the isolated particle may be a result of the interaction between the

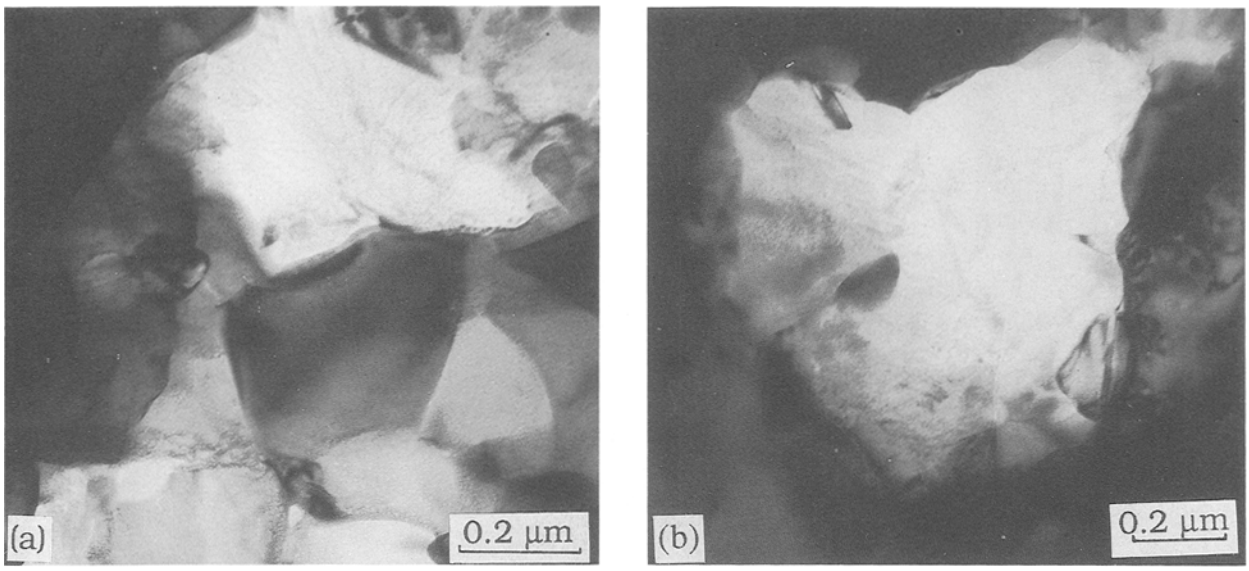

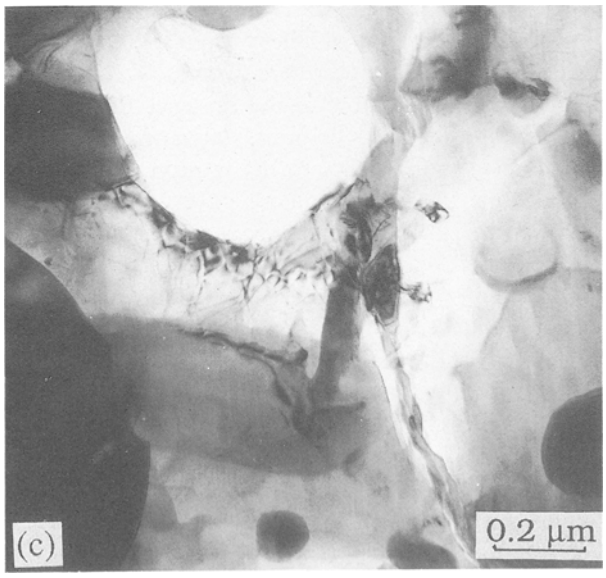

Figure 9 TEM micrographs taken from transverse sections of the extrudate (375 °C): (a) a general microstructure containing deformed and recrystallized grains; (b) a recrystallized grain, and (c) a new grain in the vicinity of an original powder particle boundary.

particle and the growing grain boundary, proceeding essentially in a static manner. Nevertheless, from the observation of the microstructure on the transverse sections, it is clear that recrystallization, either dynamic or meta-dynamic, occurred in the material. The longitudinal microstructure of the extruded material, as will be shown later, provides firm proof that dynamic recrystallization did occur during extrusion.

It is generally understood that aluminium has a high stacking fault energy, which facilitates recovery to occur by dislocation cross-slip and climb. Dynamic recovery is, therefore, the most often observed mode of restoration in aluminium alloys [16]. The observation of recrystallization in the present alloy may first be attributed to the involvement of magnesium which is known to promote dynamic recrystallization. It has been reported that, with a rise of magnesium content from 5 to 10% in aluminium, dynamic recrystallization becomes increasingly important [27, 28]. In the present alloy, however, the amount of magnesium is unlikely to be capable of modifying the deformation mode of the material to such an extent and thus this factor is not a major one. A more important factor that can account for the observation is the presence of high volume fractions of the non-deformable silicon crystals and multi-phase dispersoids in the material, which will lead to inhomogeneous deformation of the aluminium matrix and thus stimulate the nucleation of recrystallization to occur in their vicinities [29]. Such a stimulating role of dispersed phases has also been found in an Al–Si–Fe–Cu–Mg alloy produced by powder metallurgy [30] and in an Al–Si–Fe alloy processed from an Osprey preform [31]. An additional factor which should also be taken into consideration is the effect of the original powder particle boundaries. Fig. 9c shows an unbroken original powder particle boundary, and adjacent to that is a fine equiaxed grain. The micrograph was taken at the centre of the extrudate where the material underwent the least shearing to break up and redistribute the oxides on the original powder particle boundaries. The stimulation of recrystallization by the original powder particle boundaries has never been reported in other rapidly solidified aluminium alloys, but it has been repeatedly observed in the present extruded material in hot torsion tests, which will be reported in a forthcoming communication. It should be recalled that the original powder particles atomized in air are covered by an oxide layer with an average thickness of 30–33 nm [4]. This layer should mostly be broken up and redistributed by repeated shearing in the deformation zone of extrusion so as to become discrete oxides, usually indistinguishable from fine precipitates or dispersoids. Due to the inherent non-uniformity of shearing across the deformation zone, at the centre, the original powder particle boundaries may not be completely destroyed. During the concurrent deformation, the retained boundaries will block free motion of dislocations from one original powder particle to another so that high stress concentrations will occur. When the local, inhomogeneous strains are high enough, recrystallization will nucleate in their vicinities.

Observed from longitudinal sections of the material extruded under the same conditions, the microstructure was mostly composed of elongated grains with substructure (Fig. 10a), but some equiaxed grains were also present. The latter showed clear evidence that they were formed dynamically during extrusion. Fig. 10b illustrates a recrystallized grain with clear internal microcells which are gradually less visible from the lower to the upper side. It may be assumed that the grain was formed just before the termination of deformation. While growing from the lower to the upper side, the new grain was subject to continuing deformation, resulting in the creation of new substructure (microcells). It was noted that, in the recrystallized grain, there existed no internal particles to prohibit its growth, but further to the upper side, the growth was affected by a resident particle, resulting in the bulging of the grain boundary. This clearly illustrates that the growth of the recrystallized grain was only permitted in the particle-free regions.

Fig. 10c shows a typical example of the newly formed microcells within a recrystallized grain. It can clearly be seen that the cells with low misorientations have been elongated in the direction of growth, leading to a brick-like morphology. These microcells are a preform of subgrains which are expected to develop as further deformation proceeds. This is definitely proof that dynamic recrystallization occurred during the extrusion of the present alloy, according to the criteria proposed for judging the static and dynamic recrystallization [16]. It can be concluded that, in the present alloy, restoration proceeded in both dynamic recovery and dynamic recrystallization modes during extrusion. As reasoned earlier, the modification from the sole dynamic recovery in conventional aluminium alloys to the additional involvement of dynamic recrystallization in the present alloy is attributed principally to high volume fractions of the silicon crystals and multi-phase dispersoids with various sizes, as well as to the retained original powder particle boundaries with oxides. The observed operation of dynamic recrystallization appears to be in agreement with the significant change of external pressure during extrusion, as reported earlier. At the initial stage of extrusion, the compacted billet was greatly work hardened up to a peak value where dynamic recovery was activated. However, due to the presence of high volume fractions of the silicon crystals and dispersoids, which acted as obstacles to the motion of generated dislocations, the completion of recovery was inhibited. In the mean time, inhomogeneous strains around the obstacles were accumulated to promote the nucleation of dynamic recrystallization. The combined onset of dynamic recovery and recrystallization led to a large stress relief of the material, and thus a large reduction of extrusion pressure over the peak.

The nickel-containing dispersoid and Mg_2Si precipitate particles were observed to be abundant in the extruded material. They were morphologically indistinguishable. Many of them were aligned in the elongated grains (Fig. 11a). Their interspacing varied greatly within each grain and between grains. The

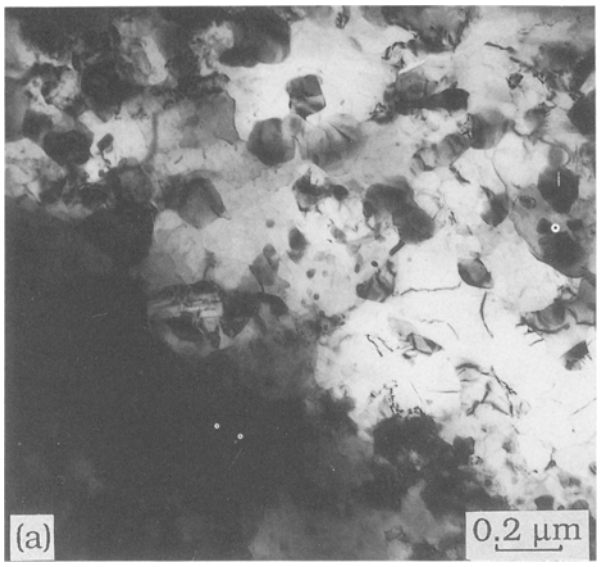

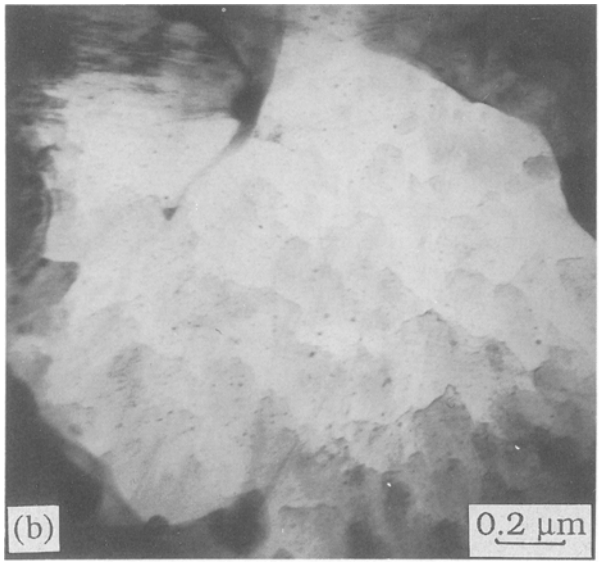

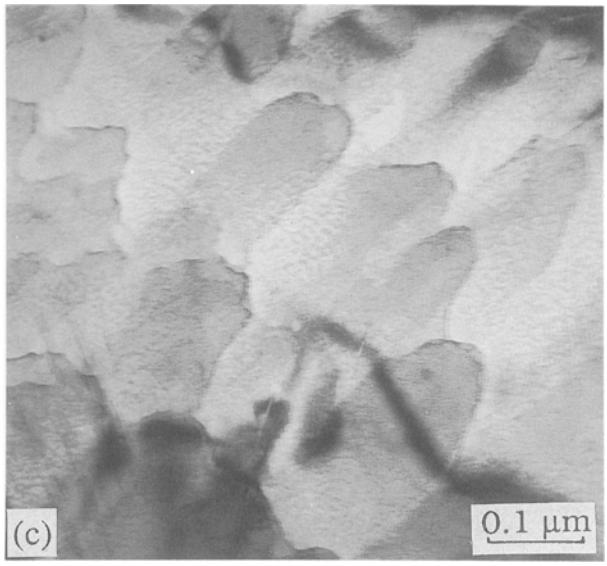

Figure 10 TEM micrographs taken from longitudinal sections of the extrudate (375 °C): (a) a worked microstructure; (b) a dynamically recrystallized grain, and (c) microcells in a dynamically recrystallized grain.

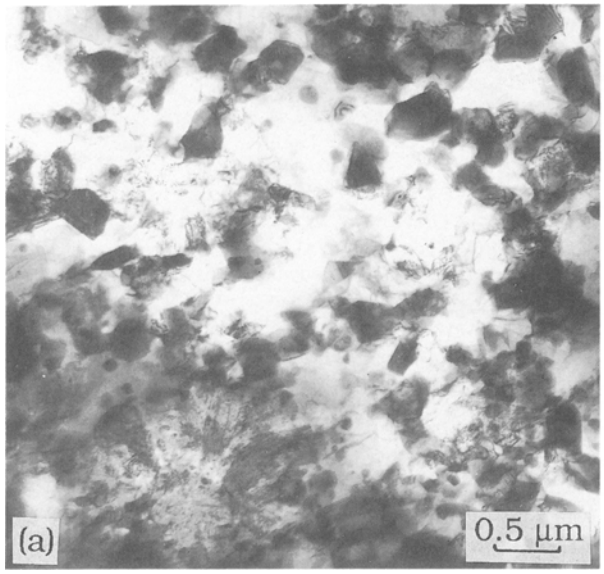

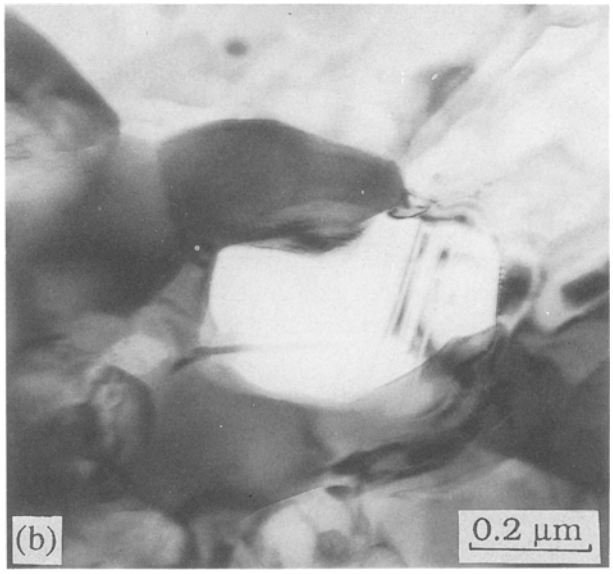

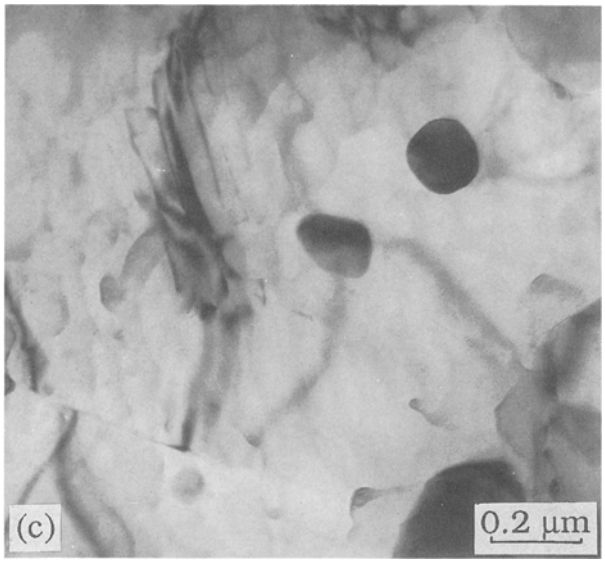

Figure 11 TEM micrographs taken from longitudinal sections of the extrudate (375 °C): (a) precipitates in elongated grains; (b) restriction to the growth of a recrystallized grain, and (c) precipitates in a worked grain with internal dislocations.

inhomogeneity of their distribution is an important cause for the formation of the partially recovered and partially recrystallized microstructure. In most of the recrystallized grains, internal particles were found to be absent. The new grains were nucleated in the vicinities of the internal particles, but their growth was constrained by the particles, as shown in Fig. 11b. In the particle-populated areas, the worked structure was retained, implying that the recrystallization was suppressed there. Moreover, in the worked subgrains, very fine particles were associated with microcells and dislocations, inhibiting the completion of recovery, as shown in Fig. 11c. It is, therefore, evident that the multi-phase dispersoids and silicon crystals formed before and probably during deformation played a very complicated role resulting in the inhomogeneous, duplex microstructure of the extruded material.

An increase in extrusion temperature did not produce a subgrain structure with an increased size. This is probably due to the existence of a spectrum of subgrain sizes in the material, which prevents the visibility of the influence of the extrusion temperature. Only observable from longitudinal-section microstructures was that the volume fraction of equiaxed, recrystallized grains increased with rising extrusion temperature. The distinction between the dynamically and statically recrystallized grains in the material extruded at 450 °C was not as clear as that shown in the material extruded at the lower temperatures. The reason is that the operation of dynamic restoration is favoured by a higher temperature and therefore the worked structure will contain less dislocations and recrystallized grains contain less substructures. Furthermore, it is known that, when dynamic recrystallization is a deformation mode, meta-dynamic and static recrystallization can easily follow [27]. The recrystallized grains were observed to be non-uniform in size depending on the interspacing of the internal particles. Their variation in size with extrusion temperature was unclear, which makes it impossible to determine a definite correlation between the as-extruded microstructure and extrusion temperature.

4. Conclusions

1. The extrusion of the Al–20Si–7.5Ni–3Cu–1Mg powder alloy was characterized by a high pressure requirement and a very large pressure drop over a peak value, which has been considered to be caused by massive internal obstacles to resist metal flow and by the occurrence of dynamic recovery and recrystallization in the material, respectively. The variation of the peak extrusion pressure with temperature can be described with the temperature-compensated strain rate.

2. The material exhibited a narrow extrudable range of process parameters: a low temperature (325 °C) prevented the successful operation of extrusion, while a high temperature (475 °C) resulted in incipient melting; a low reduction ratio (5:1) could not deform very fine powder particles, while a high reduction ratio (60:1) produced discontinuous stringers of cracked, block-like silicon crystals.

3. The combination of temperature and deformation in hot consolidation brought about the decomposition of the meta-stable aluminium matrix formed during atomization. This was revealed by the changes in the peak angle and breadth of the X-ray diffraction lines from the aluminium matrices before and after extrusion, resulting from the precipitation of supersaturated solutes. These two X-ray diffraction characteristics varied systematically with extrusion temperature, which has been explained by the effects of the retained solutes and unrelieved stresses in the aluminium matrices.

4. The transformations of intermetallic compounds were also observed by comparing X-ray diffraction patterns before and after extrusion. Three nickel-containing phases, Al_3Ni, $Al_3(NiCu)_2$ and Al_7Cu_4Ni, and a Mg–Si precipitate were found in the extruded material, irrespective of extrusion temperature. This, in combination with the results obtained from thermal analysis, suggests that their formation was assisted by deformation.

5. Hot extrusion led to a significant change in the morphology of the silicon crystals in the alloy. Their coarsening at high extrusion temperatures was not observable, which has been explained in terms of the blockade of the diffusion paths by the thermally stable nickel-containing dispersoids.

6. The as-extruded aluminium matrix showed a duplex microstructure consisting of dynamically recovered and recrystallized grains. The modification in deformation mode is attributable to the presence of the silicon crystals and multi-phase dispersoids with various sizes. The stimulation of recrystallization by the original powder particle boundaries was also observed. Due to the non-uniformity in the sizes of grains and subgrains, no systematic correlation between the extrusion conditions and resultant microstructure could be defined.

Acknowledgements

The authors would like to thank the Showa Denko K. K., Japan, for supplying the powder used as the raw material in this work. Thanks are also extended to Ing. N. M. van der Pers and Ing. E. J. A. van Dam for their help with X-ray diffraction and SEM analyses, respectively. Financial support from the Program of Innovative Research (IOP) in the Netherlands is gratefully acknowledged.

References

1. T. HIRANO, F. OHMI, S. HORIE, F. KIYOTO and T. FUJITA, in Proceedings of the International Conference on Rapidly Solidified Materials, California, February 1986, edited by P. W. Lee and R. S. Carbonara (ASM, Metals Park, Ohio, 1986) p. 327.
2. N. AMANO, Y. ODANI, Y. TAKEDA and K. AKECHI, *Metal Powder Report* **44** (1989) 186.
3. J. ZHOU, J. DUSZCZYK and B. M. KOREVAAR, *J. Mater. Sci.* **27** (1992).
4. J. L. ESTRADA and J. DUSZCZYK, *ibid.* **25** (1990) 886.
5. J. ZHOU and J. DUSZCZYK, *J. Mater. Shaping Technol.* **6** (1989) 241.
6. E. K. IOANNIDIS and T. SHEPPARD, *Mat. Sci. Technol.* **6** (1990) 749.
7. M. A. ZAIDI, *Mater. Sci. Eng.* **98** (1988) 221.
8. H. JONES, *ibid.* **5** (1969/1970) 1.
9. J. ZHOU, J. DUSZCZYK and B. M. KOREVAAR, *J. Mater. Sci.* **26** (1991) 3292.
10. E. J. MITTEMEIJER, P. VAN MOURIK and TH. H. DE KEIJSER, *Phil. Mag. A.* **43** (1981) 1157.
11. M. F. SINGLETON, J. L. MURRAY and P. NASH, in "Binary Alloy Phase Diagrams", Vol. 1, edited by T. B. Massalski (ASM, Metals Park, Ohio, 1986) p. 140.
12. L. F. MONLDOFO, in "Aluminium Alloys, Structure and Properties" (Butterworths, London, 1976) pp. 509, 566 and 604.
13. L. A. WIILLEY, in "Metals Handbook", 8th Edn, Vol. 8 (ASM, Metals Park, Ohio, 1973) p. 397.
14. D. L. W. COLLINS, *J. Inst. Metals* **86** (1957/58) 325.
15. P. GUYOT and M. WINTENBERGER, *J. Mater. Sci.* **9** (1974) 614.
16. M. A. ZAIDI and J. A. WERT, in "Treatise on Materials Science and Technology, Aluminium Alloys—Contemporary Research and Applications", Vol. 31, edited by A. K. Vasudevan and R. D. Doherty (Academic Press, Boston, 1989) p. 137.
17. F. A. SHUNK, in "Constitution of Binary Alloys, Second Supplement" (McGraw-Hill, New York, 1969) p. 495.
18. A. TONEJC, D. ROCAK and A. BONEFACIC, *Acta Metall.* **19** (1971) 311.
19. K. CHATTOPADHYAY, P. RAMACHANDRARAO, S. LELE and T. R. ANANTHARAMAN, in Proceedings of the 2nd International Conference on Rapidly Quenched Metals, The Massachusetts Institute of Technology, November 1975, edited by N. J. Grant and B. C. Giesen (The Massachusetts Institute of Technology, Boston Massachusetts, 1976) p. 157.
20. J. H. PEREPEZKO and D. U. FURRER, in Proceedings of a Symposium on Dispersion Strengthened Aluminium alloys at the 1988 TMS Annual Meeting, Phoenix, Arizona, January 1988, edited by Y. W. Kim and W. M. Griffith (TMS, Warrendale, Pennsylvania, 1988) p. 77.
21. N. NISHI, S. KAMI, Y. TAKAHASHI, H. KOMOTO and J. G. CONELY, *ibid.* p. 451.
22. E. R. PETTY, *J. Inst. Metals* **8** (1960/61) 343.
23. E. A. STARKE, Jr and J. A. WERT, in Proceedings of a Symposium on Aluminium Powder Metallurgy at the 1985 TMS/AIME Fall Meeting, Toronto, Canada, October 1985, edited by G. J. Hildeman and M. J. Koczak (The Metallurgical Society of AIME, Warrendale, Pennsylvania, 1986) p. 3.
24. M. HANSEN, in "Constitution of Binary Alloys", 2nd Edn (McGraw-Hill, New York, 1958) p. 118.
25. J. ZHOU and J. DUSZCZYK, in Proceedings of the 1st European Conference on Advanced Materials and Processes, Aachen, Germany, November 1989, edited by H. E. Exner and V. Schumacher, Vol. 1 (DGM Informationsgesellschaft-Verlag, Oberursel, 1990) p. 241.
26. J. ZHOU, J. DUSZCZYK and B. M. KOREVAAR, *J. Mater. Sci.* **26** (1991) 3041.
27. T. SHEPPARD and M. G. TUTCHER, *Metal Sci.* **14** (1980) 579.
28. T. SHEPPARD, M. A. ZAIDI and G. H. TAN, *ibid.* **17** (1983) 563.
29. F. J. HUMPHREYS, *Acta Metall.* **25** (1977) 1323.
30. J. ZHOU, J. DUSZCZYK and B. M. KOREVAAR, *J. Mater. Sci.* **26** (1991) 824.
31. *Idem, ibid.* **26** (1991) 5275.

Received 25 March
and accepted 24 April 1991